3

Development of Resonant Magnetic Field Microsensors: Challenges and Future Applications

Agustín L. Herrera-May[1,2], Luz A. Aguilera-Cortés[2],
Pedro J. García-Ramírez[1], Nelly B. Mota-Carrillo[1],
Wendy Y. Padrón-Hernández[1] and Eduard Figueras[3]
[1]*Centro de Investigación en Micro y Nanotecnología, Universidad Veracruzana*
[2]*Departamento Ingeniería Mecánica, Universidad de Guanajuato*
[3]*Instituto de Microelectrónica de Barcelona/CSIC*
[1,2]*Mexico*
[3]*Spain*

1. Introduction

Microelectromechanical Systems (MEMS) integrate electrical and mechanical components with feature sizes in the micrometer-scale, which can be fabricated using integrated circuit batch-processing technologies (Gad-el-Hak, 2001). The development of devices using MEMS has important advantages such as small size, light weight, low-power consumption, high sensitivity and high resolution (Herrera-May et al., 2009a). MEMS have allowed the development of several microdevices such as accelerometers (L. Li et al., 2011), gyroscopes (Che et al., 2010), micromirrors (Y. Li et al., 2011), and pressure sensors (Mian & Law, 2010). Recently, some researchers (Mohammad et al., 2010, 2011a, 2011b; Wang et al., 2011) have integrated acceleration, pressure or temperature sensors using MEMS. A potential market for MEMS will include magnetic field microsensors for applications such as automotive industry, telecommunications, medical and military instruments, and consumer electronics products (Lenz & Edelstein, 2006).

The most sensitive magnetic field sensor is the Superconducting Quantum Interference Device (SQUID), which has a resolution on the order of several femptoteslas (Josephs-Franks et al., 2003). It operates at low temperature based on two effects: flux quantization and Josephson effects. This sensor needs a sophisticated infrastructure that increases its size and cost, which limits its commercial applications.

Hall effect sensors have a low cost, small size, and a power consumption from 100 to 200 mW. They are fabricated on standard Complementary Metal-Oxide Semiconductor (CMOS) technology and can measure either constant or varying magnetic field between temperature ranges from -100 to + 100 ºC (Ripka & Tipek, 2007). Nevertheless, Hall effect sensors have a low resolution from 1 to 100 mT and require temperature compensation circuits (Popovic, 2004). Fluxgate sensors can measure static or low frequency magnetic field with a resolution of 100 pT (Ripka & Tipek, 2007). They have a size of several millimeters and a power

consumption close to 100 mW. These sensors require a complex fabrication of the magnetic core and coils (Baschirotto, 2006); in addition, the reduction of their mass and power decreases both their sensitivity and stability (Diaz-Michelena, 2009). In order to miniaturize fluxgate sensors is needed to solve two problems: the miniaturization of the coils and the integration of the magnetic core (Perez et al., 2004).
Anisotropic Magnetoresistive (AMR) sensors have a resolution of 10 nT, a size on order of millimetres, and a power consumption of a few milliwatts (Ripka, 2000). AMR sensors employ the anisotropic magnetoresistive effect of ferromagnetic transition metals, whose electrical resistance depends on the angle between the electrical current and the direction of magnetization. However, these sensors require a complex resetting procedure and are saturated at low magnetic fields (close to several milliteslas).
Giant Magnetoresistive (GMR) sensors can detect magnetic fields form 10 to 10^8 nT (Lenz & Edelstein, 2006) and have a size close to 1 mm. They suffer a large change in the electrical resistance when a magnetic field is applied on their thin layers of ferromagnetic and non-magnetic materials. GMR sensors can be damaged under magnetic fields close to 1 T and have higher both temperature dependence and offset than AMR sensors (Ripka, 2008).
Fiber optic sensors can detect magnetic fields from 10^{-2} to 10^6 nT and are immune to Electromagnetic Interference (EMI) (Bahreyni, 2006). These sensors exploit the magnetostrictive effect, which changes the dimensions of the magnetostrictive material under an external magnetic field. The magnetostrictive material is bonded over a piece of optical fiber that operates as a Mach-Zender interferometer. It measures the strain of the optical fiber under an external magnetic field. Unfortunately, fiber optic sensors are affected by both temperature and pressure shifts.
Resonant magnetic field microsensors based on MEMS are a new alternative in order to detect magnetic fields with a resolution close to nanoteslas (Herrera-May et al., 2009a). These microsensors employ resonant structures for monitoring magnetic fields through Lorentz force and use capacitive, piezoresistive or optical sensing techniques. They offer advantages such as a small size (on order of micrometers), low power consumption (around of milliwatts), high functionality, wide dynamic range, and low cost through batch fabrication. They can be more compact and lighter than the SQUIDs, fiber optic sensors, and search coil sensors. Magnetic field sensors based on MEMS can be placed closer to low-magnetic field sources in order to increase their output signals. These sensors need to be subjected to more studies of reliability in order to guarantee a safe operation in future commercial market. Several of they have problems such as nonlinear response, necessity of vacuum packaging, post-processing steps for releasing their resonant structures, and complex signal conditioning circuits.
This work presents the development of resonant magnetic field microsensors based on MEMS that exploit the Lorentz force principle. It describes the general performance, advantages, drawbacks, challenges and future applications of the resonant magnetic field microsensors.

2. Development of resonant magnetic field microsensors

This section presents the development of several resonant magnetic field microsensors based on MEMS. It describes the general performance and sensing techniques of these microsensors.

2.1 Operation principle and materials

This section describes the general performance of resonant magnetic field microsensors. A resonant magnetic field microsensor uses a resonant structure in order to detect external magnetic fields. Due to the resonant structure, the sensitivity of this sensor can be increased by a parameter equal to its quality factor. The structure of the magnetic field microsensor is excited at its fundamental resonant frequency through Lorentz forces or electrostatic forces. Generally, this structure is integrated by beams and/or plates, which are fabricated using surface or bulk micromachining. An external magnetic field alters the deflections of the resonant structure that can be measured by means of capacitive, piezoresistive or optical sensing techniques.

Figure 1 shows the SEM image of a resonant magnetic field microsensor formed by thin silicon beams and a Wheatstone bridge with four p-type piezoresistors. It has been developed by the MEMS group from the Research Center for Micro and Nanotechnology (MICRONA) of the Veracruzana University into collaboration with the Microelectronics Institute of Barcelona (IMB-CNM, CSIC). This microsensor exploits the Lorentz force and uses a piezoresistive sensing technique. It has a silicon structure that oscillates at its first resonant frequency under an external magnetic field, as shown in Fig. 2(a). A Lorentz force is generated by the interaction between an external magnetic field B_x (parallel a length of the resonant structure) and a sinusoidal excitation current (I_e) flowing through an aluminium loop. The Lorentz force is given by

$$F_L = I_e L_y B_x \tag{1}$$

$$I_e = \sqrt{2} I_{RMS} \sin(2\pi f t) \tag{2}$$

where I_{RMS} is the root-mean square (RMS) of I_{Al}, L_y is the overall wide of the aluminium loop perpendicular to B_x, t is the time and f is the frequency.

The Lorentz force causes a bending moment on the resonant structure, which strains four bending beams as well as two piezoresistors placed on them. The maximum bending moment (M_{max}) and longitudinal strain (ε_L) over these beams are calculated as

$$M_{\max} = 2F_L L_x \tag{3}$$

$$\varepsilon_l = \frac{3M_{\max}}{2Ebh^2} Q \tag{4}$$

where L_x is the distance between a free end of the aluminum loop to the connection point of a bending beam with the supporting beam, Q is the quality factor of the resonant structure, E is the elastic modulus of the silicon, b and h are the width and thickness of the bending beam, respectively.

The longitudinal strain (ε_l) modifies the initial resistances (R_i) of two piezoresistors, which changes the output voltage (V_{out}) of the Wheatstone bridge (see Fig. 2(b)). The V_{out} can be determined as

$$V_{out} = \frac{\Delta R_i}{2R_i} V_{bias} \tag{5}$$

where ΔR_i is the resistance variation of the piezoresistors and V_{bias} is bias voltage of the Wheatstone bridge.
Thus, the magnetic input signal is converted to an electrical output signal through the Wheatstone bridge.

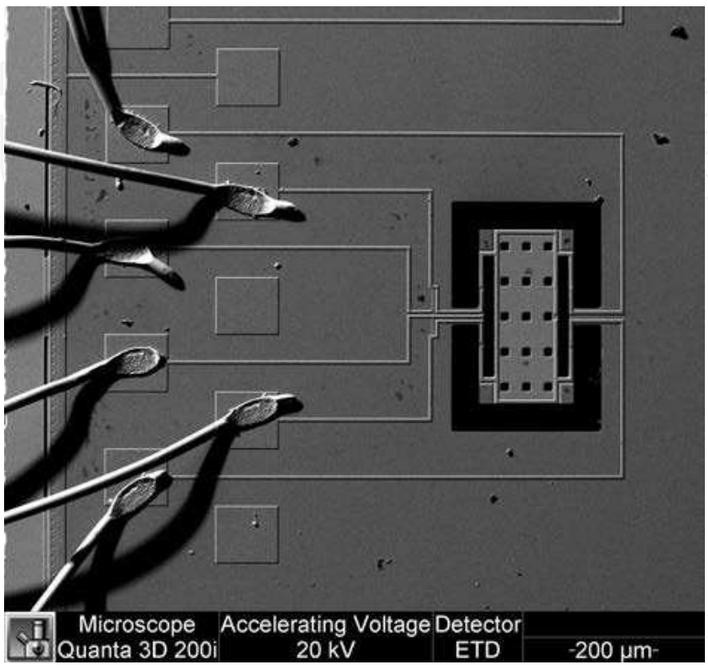

Fig. 1. SEM image of a resonant magnetic field microsensor based on MEMS.

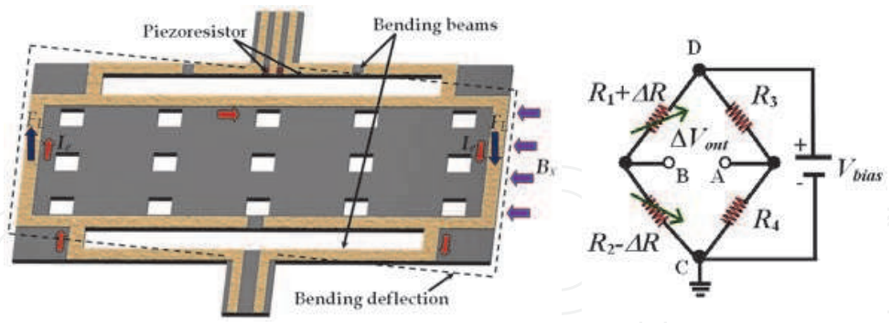

Fig. 2. A schematic view of the (a) operation principle of a resonant magnetic field microsensor with piezoresistive detection and (b) its associated Wheatstone bridge.

For the two piezoresistors under a longitudinal strain (ε_l), their ΔR_i is determined by (Clark and Wise, 1979)

$$\frac{\Delta R_i}{2R_i} = \pi_l E \varepsilon_l \tag{6}$$

where π_l is the piezoresistive coefficient parallel to the piezoresistor length.

The sensitivity (S) of the resonant magnetic field microsensor can be determined as the ratio of the output voltage (V_{out}) to the range of the external magnetic field (ΔB_x).
The sensitivity of the microsensor is limited by the quality factor of its resonant structure. The quality factor is defined as the ratio of the total energy stored in the resonant structure (E_T) to the energy lost per cycle (E_C) due to the damping effect:

$$Q = 2\pi \frac{E_T}{E_C} \tag{7}$$

The quality factor of the resonant structure depends of three damping sources (Beeby et al., 2004): a) energy lost to surrounding fluid; b) energy dissipated internally within the material of the resonant structure; and c) energy coupled through the structure's support to a surrounding solid.
Quality factor (Q_f) related to energy dissipated to surrounding fluid depends on the type of the fluid, vibration mode of the structure, fluid pressure, size and shape of the resonant structure, and its distance (gap) respect to adjacent surfaces. Q_f increases significantly when the fluid pressure decreases to magnitudes close to vacuum (Li & Fang, 2009). At atmospheric pressure, Q_f of the resonant magnetic field microsensor is due to the interactions of its resonant structure with the air.
Thermoelastic damping is the principal source of internal energy loss inside the material of the magnetic field microsensor. The oscillating strain gradient due to the vibration of microsensor's structure generates an oscillating temperature gradient. This temperature gradient causes a thermal energy loss known as thermoelastic damping (Vangallatore, 2005; Tunvir et al., 2010). The quality factor (Q_i) related to this damping is dominant when the resonant structure operated close to vacuum.
Quality factor (Q_l) due to support damping of the resonant structure represents the vibration energy dissipated by transmission through its support. The bending vibration of the resonant structure generates both vibrating moment and shear force on its clamped ends that excite elastic waves propagating into the supports (Hao et al., 2003). The supports of the resonant structure absorb part of the vibration energy.
Total quality factor (Q_T) of the resonant magnetic field microsensor can be obtained as

$$\frac{1}{Q_T} = \frac{1}{Q_f} + \frac{1}{Q_i} + \frac{1}{Q_l} \tag{8}$$

Most of the resonant magnetic field microsensors have been fabricated using silicon and polysilicon materials. The mechanical properties of these materials are affected by variations in their temperature. For instance, the silicon elastic modulus E(T) as function of the temperature from 250 K to 1500 K can be expressed as (Hull, 1999)

$$E(T) = E_i\left(1 - 9.4 \times 10^{-5} T\right) \tag{9}$$

where E_i is the elastic modulus of silicon at room temperature and T is the temperature in Kelvin.
The thermal expansion coefficient of silicon (α_{Si}) for temperature range from 293 K to 1025 K can be determined as (Watanable, 2004)

$$\alpha_{Si}(T) = -3.0451\times10^{-6} + 0.035705\times10^{-6}T - 7.981\times10^{-11}T^2 + 9.5783\times10^{-14}T^3 - 5.8919\times10^{-17}T^4 + 1.4614\times10^{-20}T^5 \quad (10)$$

The thermal conductivity of silicon (k_{Si}) for temperature range from 300 K to 400 K can be obtained as (Hull, 1999)

$$k_{Si}(T) = 309 - 0.51T \quad (11$$

Temperature fluctuations affect the elastic modulus, thermal expansion coefficient, and thermal conductivity of silicon. Thus, the fundamental resonant frequency of a magnetic field microsensor changes when its elastic modulus is modified. In addition, temperature shifts cause internal stresses on the resonant structure, which alter its resonant frequency. High temperatures may generate wear-out, corrosion, and performance degradation of a resonant structure (Darrin, 2006). Therefore, the temperature control is important issue in order to obtain a stability in the fundamental frequency of the magnetic field microsensor. It can be got through compensation electronic circuits.

2.2 Capacitive sensing

This section presents several resonant magnetic field microsensors based on MEMS that use capacitive sensing techniques.

Kádár et al. (1998) developed a resonant magnetic field microsensor with capacitive sensing. It was fabricated using a combination of bipolar processing, micromachining, glass processing and glass-to-silicon anodic bonding. This microsensor consists of a resonant silicon plate (2800× 1400 μm) with electrodes and a rectangular coil deposited on its surface. The interaction of an external magnetic field with a sinusoidal current generates a Lorentz force that causes a seesaw motion of the silicon plate. The seesaw motion modifies the distance (gap) between the silicon plate and the electrodes located into its packaging, which changes the capacitance value. Thus, the magnetic field signal is related with the capacitance shift detected by the electrodes. This microsensor can reach a resolution of 1 nT, but requires a vacuum packaging and a complex electronic circuit for the signal processing. For a single loop, it has a sensitivity of 500 μV$\mu\cdot$T^{-1}, a resonant frequency close to 2.4 kHz, a quality factor of 700 at 5 Pa, and a power consumption of a few milliwatts.

Emmerich and Schöfthaler (2000) fabricated a resonant magnetic field microsensor using a Bosch's standard surface micromachining process. It constains a suspended polysilicon beam with movable and fixed fingers electrodes. The interaction of a current and external magnetic field displaces the suspended beam, which changes the capacitance between the movable and fixed electrodes. This capacitance shift depends of the magnitud and direction of the external magnetic field. The microsensor operates in its resonant frequency and into a vacuum ambient in order to increase its sensitivity. It presents a sensitivity of 820 μV$\cdot\mu$T^{-1} for an excitation current of 930 μA, a quality factor close to 30 at 101 Pa, a resonant frequency around 1.3 kHz, and a resolution of 200 nT considering a frequency diference of 10 Hz. This microsensor needs a vacuum packaging and a complex fabrication process. In addition, it has an offset close to 60 μT caused by the magnetic background field, voltage offsets and unbalanced parasitic capacitances.

Tucker et al. (2002) designed a xylophone microbar to detect external magnetic fields. It is the resonant structure of a magnetic field microsensor that was fabricated using a commercial 0.5

micron CMOS process. Post-CMOS processing was needed to release the xylophone microbar. Fig. 3 illustrates the operation principle of this microsensor. The microbar is supported by four arms at the nodes of its fundamental vibration mode in order to decrease the support damping. A Lorentz force is generated when a sinusoidal current flows through the microbar under an external magnetic field. This force causes a microbar vibration, which is measured capacitively. The microsensor has a die area close to 0.5 mm^2, a resonant frequency around 100 kHz, a quality factor about 1000, a power consumption of 7.5 mW, and a noise of 0.5 nT·Hz$^{-1/2}$. It must be vacuum packaging in order to increase the vibration amplitudes of the microbar.

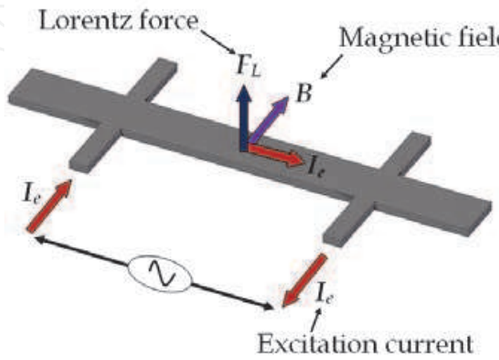

Fig. 3. Operation principle of a resonant magnetic field microsensor based on xylophone microbar proposed by Tucker et al. (2002).

Bahreyni & Shafai (2007) designed a magnetic field microsensor based on an electrostatic resonator (shuttle) fabricated in MicraGEM technology available from Micralyne Inc. The shuttle is connected to two crossbars (520 × 9 × 10 μm) by four microbeam springs (200 × 3 × 10 μm), as shown in Fig. 4. The crossbars are designed to be much stiffer in the y direction than the x direction. The shuttle is driven and kept into resonance by means of electrostatic actuation and sensing. During the microsensor operation, a DC current (I_{XB}) flowing through the crossbars. The interaction of I_{XB} with a magnetic field (B_z) normal to the microsensor's surface generates a Lorentz force (F_L) in the x direction of the crossbars. This force is axially transferred to the four microbeam springs, modifying the total stiffness of the four springs. The stiffness variation is proportional to B_z and I_{XB}, which alters the resonant frequency of the microsensor's structure. Then, the resonant frequency shift is monitored using signal processing electronics. This microsensor has a sensitivity of 69.6 Hz·T^{-1}, a resolution of 217 nT for I_{XB} equal to 10 mA, a resonant frequency close to 27 kHz, a quality factor of 15,000 at 2 Pa. Alterations in the environment temperature and the heat generated by I_{XB} affect the microsensor's performance.

Ren et al. (2009) reported a magnetic field microsensor based on a silicon resonator, which was fabricated using conventional MEMS technology and a silicon-to-glass anodic bonding process. The resonator is formed by a low-resistivity silicon plate (3000 × 2000 × 60 μm) suspended over a glass substrate by two torsional beams (500 × 20 × 60 μm), as shown in Fig. 6. This silicon plate acts as electrode of sensing capacitances, which simplifies the fabrication process of the microsensor. Au capacitance plates are fabricated on the glass substrate and a multi-turn coil (Cr and Au layers) is deposited on silicon-plate surface. A Lorentz force is generated when a sinusoidal current flows into the excitation coil under an external magnetic field. This force causes an oscillating motion of silicon plate around the

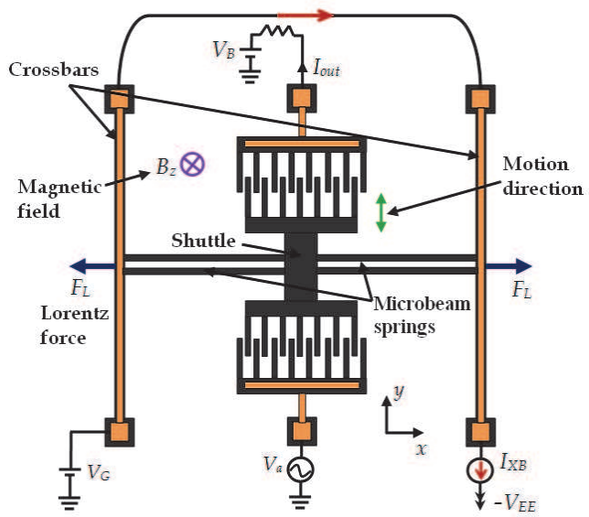

Fig. 5. Operation principle of the resonant magnetic field microsensor designed by Bahreyni & Shafai (2007).

torsional beams. This motion produces a capacitance shift between the Au electrodes and the silicon plate. A capacitance detection circuit measured the capacitance change that depends of the magnitude and direction of the external magnetic field. The microsensor needs a vacuum packaging to increase its performance. For a pressure of 10 Pa and 150 mV driving voltage amplitude, the microsensor has a resolution of 30 nT, a sensitivity of 0.40 $V \cdot T^{-1}$, a resonant frequency close to 1380 Hz, and a quality factor around 2500. Nevertheless, it presented a non-linear response from 0 to 3 μT.

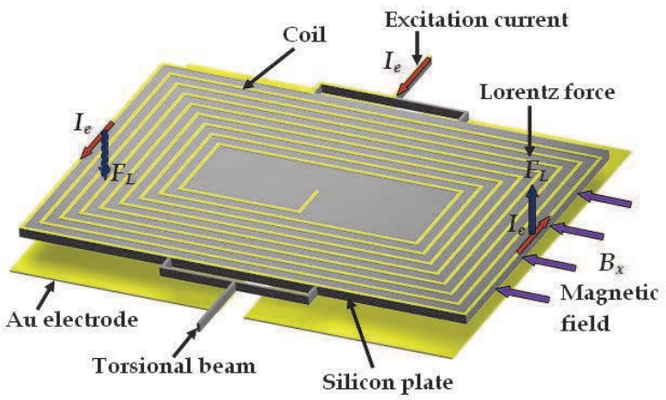

Fig. 6. Operation principle of the magnetic field microsensor designed by Ren et al. (2009).

Brugger & Paul (2009) developed a novel magnetic field microsensor (dimensions of 7.5 × 3.2 mm) integrated by an electrostatically driven silicon resonator, an amorphous magnetic concentrator, and a pair of planar coils. Interdigitated combs (200 × 14 × 25 μm) are employed for the electrostatic excitation of the resonator and the capacitive detection of its resonance (see Fig. 7). The silicon resonator is suspended by four straight flexural springs (1000 × 14 × 25 μm). The magnetic concentrator (5000 × 250 × 18 μm) is constructed using a

Metglas 2714A ribbon and is cut into three segments separated by two narrow gaps. The inner segment is attached to the resonator surface and both outer segments are fixed. The magnetic concentrator saturates to magnetic field above of 713 μT. An auxiliary magnetic field parallel to the magnetic concentrator is generated with the planar coils. Each coil comprises 12 windings with a linewidth of 55 μm and a line-to-line spacing of 15 μm. The resonator is excited at its resonant frequency applying a dc voltage (V_{dc}) to it and ac voltage (V_{ac}) to the half of the interdigitated combs. Its oscillating motion is monitoring using the other half of the interdigitated combs. A magnetic force acts on the resonator when an external magnetic field parallel to the magnetic-concentrator axis is applied. This force counteracts the restoring force exerted on the resonator by its four flexural springs, which decrease both the total spring constant and resonant frequency of the resonator. Then, a quadratic relationship between the resonant frequency and a magnetic field is obtained. In order to achieve a linear output signal of the microsensor, the external magnetic field is combined with an auxiliary magnetic field generated by the planar coils. For a coil current of 80 mA, V_{dc} = 20V, V_{ac} = 404 mV and a pressure of 10^{-5} mbar, this microsensor presents a sensitivity of 1.0 MHz·T^{-1}, a resolution of 400 nT, and a quality factor around 2400. It does not need a complex feedback and modulation electronics; however, it requires a vacuum packaging and a complex fabrication process. This process combines the following: 1) MEMS technology based on a silicon-on-insulator (SOI) substrate for the MEM structure; 2) the epoxy-resin-based attachment of a thin amorphous magnetic ribbon subsequently structured using wet chemical etching; and 3) micropatterning of the magnetic concentrator by UV-laser.

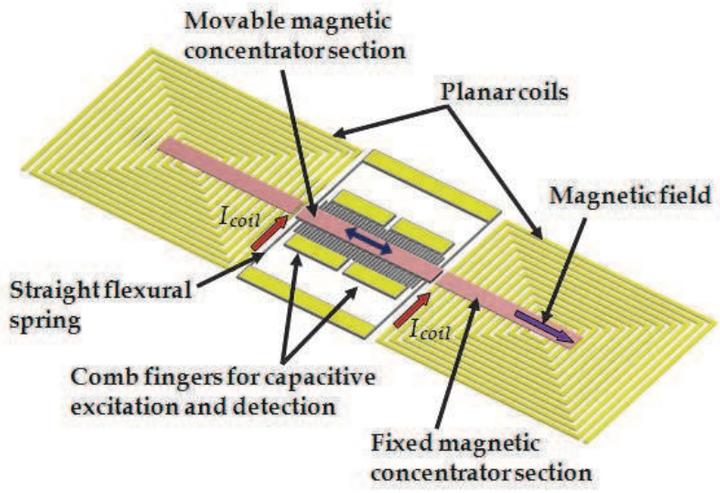

Fig. 7. Operation principle of a magnetic field microsensor based on a magnetic concentrator developed by Brugger & Paul (2009).

Generally, a resonant magnetic field microsensor with capacitive detection needs a vacuum packaging in order to increase its sensitivity and resolution. It suffers from parasitic capacitances, which can be reduced through the monolithic integration of the micromachined resonators with electronic circuits.

2.3 Optical sensing

This section includes the resonant magnetic field microsensors based on MEMS that use optical sensing.

Zanetti et al. (1998) fabricated a magnetic field microsensor formed by a xylophone microbar, which is supported (at the nodes of its fundamental vibration mode) by four microbeams. The microsensor uses optical detection for measuring the deflections of the xylophone microbar under an external magnetic field parallel to its length, as shown in Fig. 8. The interaction of this field with ac excitation current (I) flowing into the microbar produces a Lorentz force that deflects the microbar. If the ac excitation current is supplied with one frequency equal to the bending resonant frequency of the microbar, then, its deflection is increased. This deflection depends of the magnitude of the external magnetic field and is measured using a miniature laser and a position sensitive detector. Thus, the magnetic signal is proportional to the deflections of the xylophone microbar. The microsensor has dimensions of 5000 × 500 × 250 μm, a quality factor close to 700, a resolution around 1 nT and a power consumption of few milliwatts.

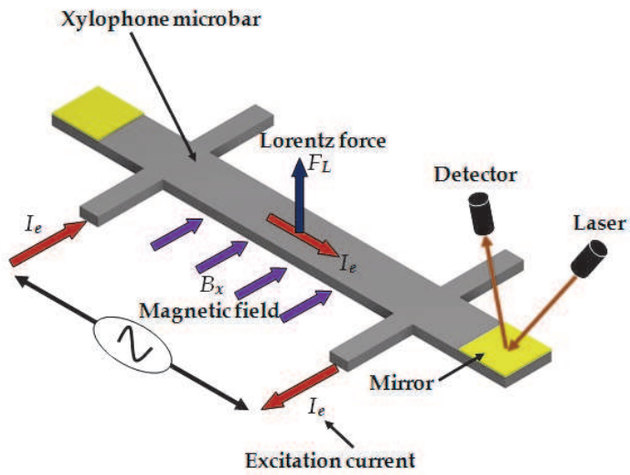

Fig. 8. Operation principle of a magnetic field microsensor with optical detection based on a xylophone microbar designed by Zanetti et al. (1998).

Keplinger et al. (2003, 2004) proposed a resonant magnetic field microsensor based on a micromachined U-shaped silicon cantilever and an optical sensing system. The cantilever (1100 × 100 × 10 μm) contains on its surface a 0.5-μm-thick Au layer, which flows an ac excitation current. A Lorentz force is generated due to the interaction of the current with a magnetic field parallel to the length of the U-shaped cantilever. This force causes a bending motion of the cantilever that is measured through optical fibers. Thus, the magnetic input signal is converted into a movement of the cantilever, which is increased when the cantilever operates at its resonant frequency. The optical sensing uses two-fiber arrangements for avoiding the problem of the interfering reflected light. In the first design the emitted light beam is reflected only once at the cantilever front side, as shown in Fig. 9. Nevertheless, it requires a large lateral space for the chip and microsensor. The second design considers a cracked cantilever to allow a parallel alignment of the fibers (see Fig. 10), which requires a perfect vertical front side of the cantilevers. This optical detection system allows the efficient transmission of the microsensor signal in an electromagnetically noisy environment. This microsensor detects magnetic fields from 10 mT to 50 T and has a resonant frequency close to 5 kHz, a quality factor of 200 at atmospheric pressure, a resolution of 10 mT, and a power consumption of a few milliwatts.

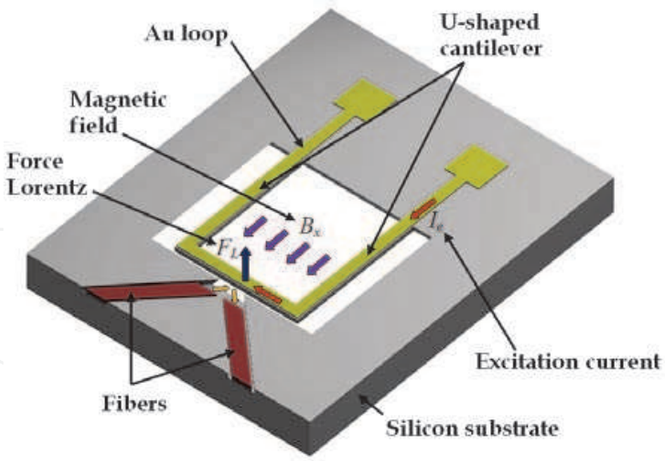

Fig. 9. Operation principle of a resonant magnetic field microsensor integrated by a U-shaped silicon cantilever and two fibers placed in curved channels, which was developed by Keplinger et al. (2003, 2004).

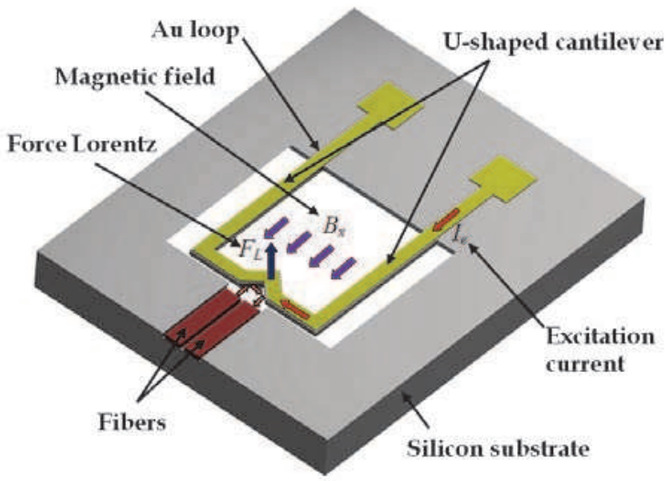

Fig. 10. Operation principle of a resonant magnetic field microsensor integrated by a U-shaped cracked cantilever and two parallel fibers, which was developed by Keplinger et al. (2003, 2004).

Wickenden et al. (2003) reported a resonant magnetic field microsensor formed by a polysilicon xylophone microbar (500 × 50 × 2 μm), which has a similar performance to microsensor designed by Zanetti et al. (1998). A magnetic input signal is converted into an oscillating motion of the xylophone microbar. This motion is detected by an optical readout system based on a laser diode beam and a position sensitive detector. This microsensor has a resonant frequency of 78.15 kHz, a quality factor around 7000 at 4.7 Pa, ac current of 22 μA, a thermal noise of 100 pT·A·Hz$^{-1/2}$, and a resolution on the order of nanoteslas. However, it presents a linear response up to 150 μT and its performance is affected by variations of pressure and temperature. The optical readout system used in resonant magnetic field microsensors allows a reduction in their electronic circuitry and weight. Furthermore, the microsensors with optical sensing have immunity to EMI.

2.4 Piezoresistive sensing

This section includes the description of several resonant magnetic field microsensors with piezoresistive sensing.

Beroulle et al. (2003) reported a magnetic field microsensor integrated by a resonant U-shaped cantilever (520 μm length and 80 μm thick), a planar aluminium coil of 8 turns, and a Wheatstone bridge of polysilicon strain gauges. This microsensor exploits the Lorentz force principle in order to measure an external magnetic field, converting it into an electrical output signal through Wheatstone bridge. The microsensor was fabricated using an industrial CMOS processes with a post-processing etch step to release its resonant structure. It has a sensitivity of 0.53 $V \cdot T^{-1}$, a theoretical resolution of 2 μT, a thermal noise of 5.3 $nV \cdot Hz^{-1/2}$, a resonant frequency of 8.97 kHz, a quality factor of 59, and a mass of 750 ng.

Sunier et al. (2006) developed a magnetic field microsensor using a resonant silicon structure, a planar aluminium coil, two heating resistors, and P-channel Metal Oxide Semiconductor (PMOS) transistors (see Fig. 11). This microsensor operates based on Lorentz force principle and provides a frequency output signal. The silicon structure vibrates at its resonant frequency because of the thermal actuation of two heating resistors. The oscillating motion of the silicon structure is detected using PMOS transistors connected in a Wheatstone bridge. A Lorentz force (generated by the interaction between an electrical current flowing through coil and an external magnetic field) changes the total spring constant of the resonant structure. This modifies the resonant frequency value of the silicon structure. Thus, the resonant frequency shift is related to the magnitude of the external magnetic field. This microsensor has an efficient continuous offset cancelation, high robustness, and low cross sensitivity. In addition, it presents a sensitivity of 60 $Hz \cdot T^{-1}$, a resolution of 1 μT, a resonant frequency of 175 kHz, a quality factor of 600, and a power consumption close to 5 mW.

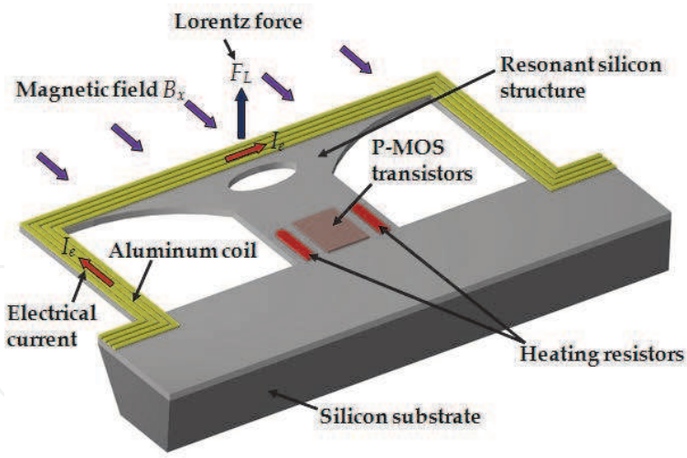

Fig. 11. Operation principle of a resonant magnetic field microsensor with frequency output designed by Sunier et al. (2006).

Herrera-May et al. (2009b) developed a resonant magnetic field microsensor with piezoresistive sensing, which contains a resonant silicon microplate (400 × 150 × 15 μm) supported by four bending microbeams, an aluminium loop, and a Wheatstone bridge of four p-type piezoresistors (see Fig. 12). It exploits the Lorentz force for monitoring external magnetic fields. This force causes an oscillating motion of the microplate and microbeams that strains two piezoresistors. This changes the piezoresistors resistance, modifying the

output voltage of the Wheatstone bridge. Then, the magnetic input signal is converted into an electrical signal. This microsensor was designed for Tenaris TAMSA Corporation for measuring residual magnetic fields in welded steel tubes. It was fabricated using the bulk micromachining technology of the Microelectronics Institute of Barcelona (IMB-CNM, CSIC). Its characteristics are: sensitivity of 0.403 $V \cdot T^{-1}$, resolution of 143 nT, resonant frequency of 136.52 kHz, quality factor of 842, and a power consumption below 10 mW. However, this microsensor presents a offset and a nonlinear response for low magnetic fields.

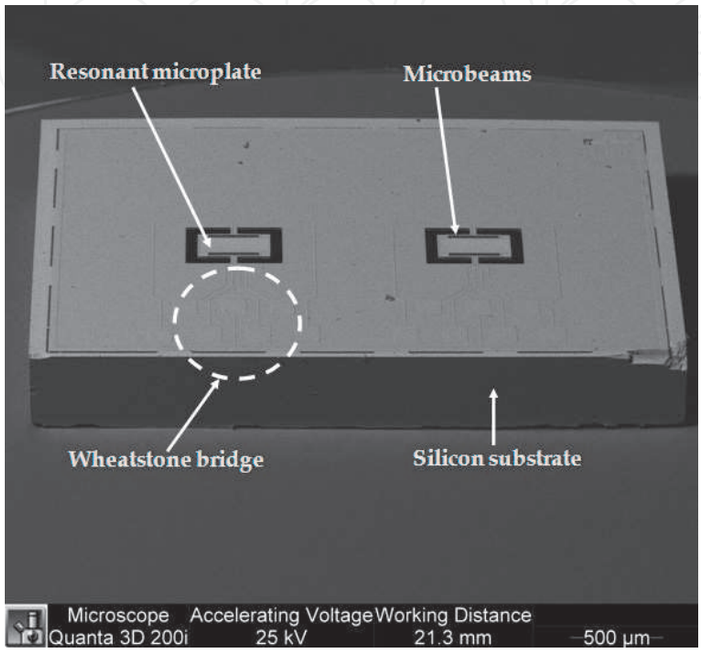

Fig. 12. SEM image of a die with two resonant magnetic field microsensors with piezoresistive sensing designed by Herrera-May et al. (2009b).

The MEMS group (Herrera-May et al., 2011) from MICRONA-UV into collaboration with IMB-CNM developed a resonant magnetic field microsensor integrated by a rectangular loop (700 × 450 × 5 μm) of silicon beams suspended with four bending beams (130 × 12 × 5 μm), an aluminium loop (1 μm thick), and four p-type piezoresistors connected into a Wheatstone bridge (see Fig. 13). This microsensor operates based on Lorentz force and has a linear response under weak magnetic fields from 40 to 2000 μT. In addition, it has sensitivity 4.8 times larger than the microsensor reported by Herrera-May et al. (2009b). This microsensor presents a resolution close to 43 nT, a resonant frequency of 22.99 kHz, a quality factor of 96.6 at atmospheric pressure, and a low power consumption of 16 mW. Later, researchers of MICRONA-UV designed other resonant magnetic field microsensor with piezoresistive sensing (see Fig. 14). It was used for monitoring magnetic fields generate by an electronic neuron developed by researchers from Institute of Physiology-BUAP (Tapia et al., 2011). This microsensor exploits the Lorentz force and is formed by an arrangement of silicon microbeams (700 × 450 × 5 μm) suspended by four bending microbeams, an aluminium loop (1 μm thick), and a Wheatstone bridge with four p-type piezoresistors. It has a compact structure, a response linear to low magnetic fields, a sensitivity of 1.2 $V \cdot T^{-1}$, a resolution of 80 nT, a resonant frequency of 13.87 kHz, a quality factor of 93 at atmospheric pressure, a power consumption of 2.05 mW, and a simple signal processing.

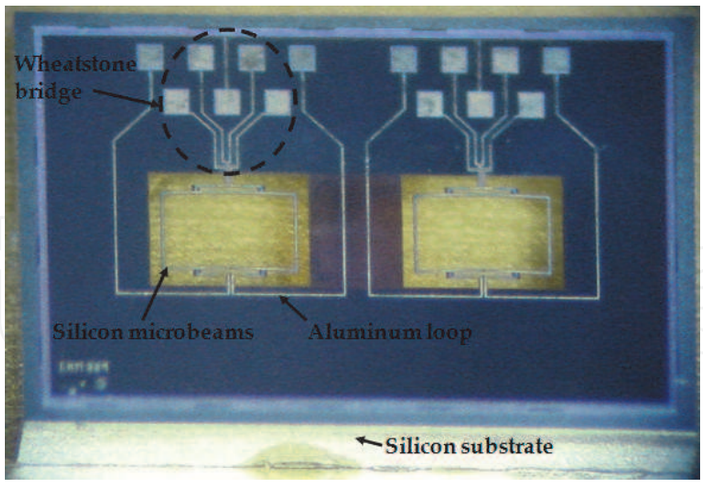

Fig. 13. Microphotograph of a die with two resonant magnetic field microsensors designed by the MEMS group of MICRONA-UV.

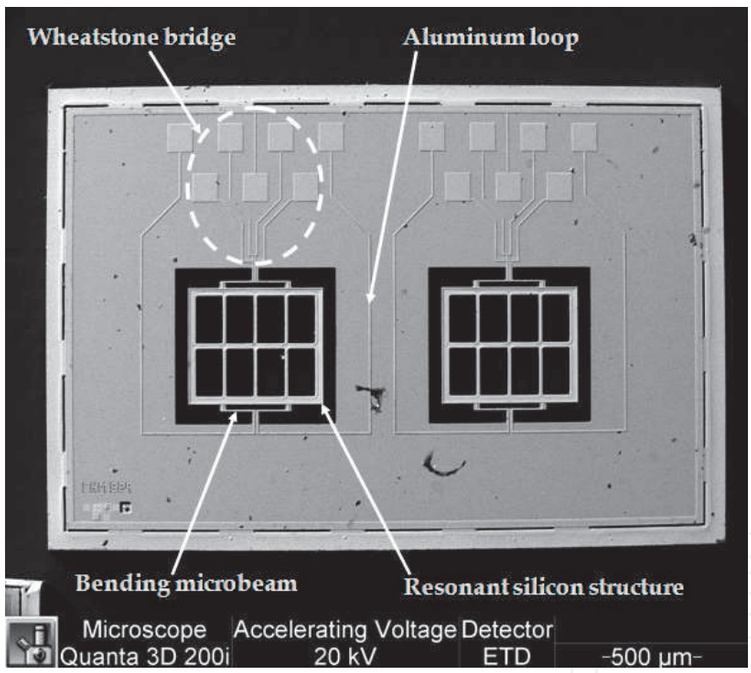

Fig. 14. SEM image of a die with two resonant magnetic field microsensors with piezoresistive detection used for neural applications (Tapia et al., 2011).

A piezoresistive sensing system used into magnetic field microsensors can allow them a simple signal processing, high sensitivity, and low-cost fabrication. Nevertheless, it is affected by temperature variations, which can be reduced through compensation circuits.

2.5 Comparison of resonant magnetic field microsensors

Most the resonant magnetic field microsensors have a compact structure, small size, and high sensitivity, wide dynamic range, and easy signal processing. Several of them can

measure low magnetic fields around nanoteslas with low consumption power. Their dynamic range can be adjusted changing the magnitude of the excitation current, allowing them to measure lower or higher magnetic fields. A comparison of the main characteristics of these microsensors are indicates in Table 1. They could compete with conventional magnetic sensors for monitoring magnetic fields with resolution on the order of nanoteslas.

Microsensor	Sensing technique	Resolution (nT)	Resonant frequency (kHz)	Quality factor	Size of resonant structure (μm × μm)
Kádár et al. (1998)	Capacitive	~1	2.40	700 @ 5 Pa	2,800 × 1,400
Emmerich & Schöfthaler (2000)	Capacitive	~200	1.30	30 @ 101 Pa	1,300 × 500
Tucker et al. (2002)	Capacitive	$<10^3$	100	~1000 @ 1 P_{atm}	<1,000 × 1,000
Bahreyni et al. (2007)	Capacitive	217	~27	15000 @ 2 Pa	~520 × 400
Ren et al. (2009)	Capacitive	30	1.38	2500 @ 10 Pa	3000 × 2000
Brugger & Paul (2009)	Capacitive	400	2.5	2400 @ 10^{-5} Pa	7500 × 3200
Zanetti et al. (1998)	Optical	1	---*	~7000 @ P_{atm}	5,000 × 500
Keplinger et al. (2003, 2004)	Optical	10^7	5	200 @ P_{atm}	1,100 × 1,000
Wickenden et al. (2003)	Optical	$<10^3$	78.15	7000 @ 4.7 Pa	500 × 50
Beroulle et al. (2003)	Piezoresistive	2×10^3	8.97	59 @ P_{atm}	520 × 520
Sunier et al. (2006)	Piezoresistive	10^3	175	600 @ P_{atm}	~400 × 185
Herrera-May et al. (2009b)	Piezoresistive	143	136.52	842 @ P_{atm}	400 × 150
Herrera-May et al. (2011)	Piezoresistive	43	22.99	96.6 @ P_{atm}	700 × 450

* Data not available in the literature

Table 1. Main characteristics of resonant magnetic field microsensors.

3. Challenges and future applications

This section considers some challenges and potential applications of the resonant magnetic field microsensors.

Future commercial markets will require the development of multifunctional sensors on a single chip for monitoring several input signals such as magnetic field, pressure, acceleration, and temperature. These sensors will be integrated by several microstructures, transducers, and electronic circuits on a same substrate using monolithic fabrication. They will have important advantages such as small size, compact structure, low power consumption, and high functionality. Therefore, the integration on a single chip of the resonant magnetic field microsensors with other type of sensors is an important challenge.

Another challenge is the suppression of any background noise in order to increase the magnetic resolution. The performance of the future magnetic field microsensors will be limited by the variations in Earth's magnetic field because of geological effects. In addition, the reduction of the output response offset and the temperature dependence of future microsensors are needed. Potential applications into the automotive industry, telecommunications, and consumer electronics products demand magnetic field microsensors

of low cost and high reliability. Also, a challenge is the optimization of their performance and the decrease of the design-phase time. Investigations on new materials with better electrical and mechanical properties than silicon could be used into the future microsensors.
Automotive industry could be a future market of the magnetic field microsensors in order to detect the speed and size of vehicles (see Fig. 15). A traffic's detection system may be formed by two microsensors (separated by 1 meter distance from each other) placed in parallel beside the road. The microsensors will measure the change of the Earth's magnetic field due to the vehicle motion, which will be proceeded to A/D converter and digital data processing system. The magnetic variation will depend of the vehicle's size and speed, and it will be detected by the microsensors in different times (t_1 and t_2). Then, the vehicle's speed will be determined through the ratio of the separation distance between the two microsensors to the time difference t_1-t_2. This system could be applied with an intelligent signal control to decrease traffic congestion on roads.

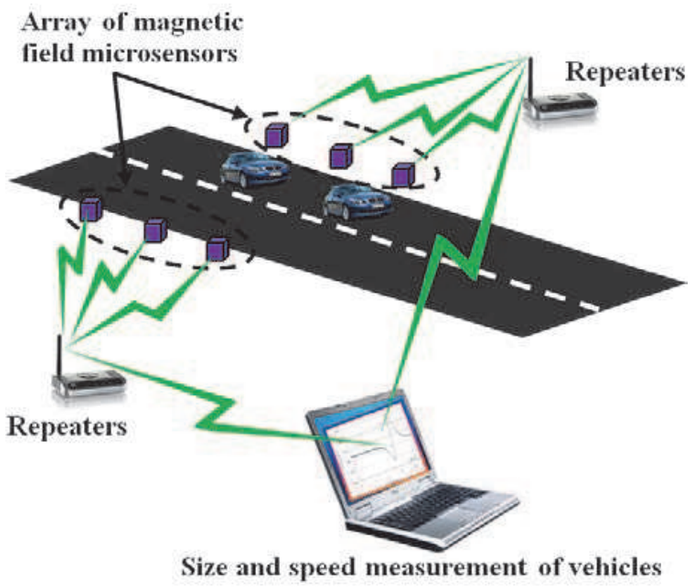

Fig. 15. Schematic diagram of a traffic's detection system based on magnetic field microsensors.

Also, magnetic field microsensors could be employed at the electronic stability program (EPS), which keeps the vehicle dynamically stable in critical situations such as hard braking and slippery surfaces. ESP systems needs data about steering-wheel angle, lateral accelerations, yaw rate, and wheel speed. These parameters could be measured through accelerations, gyroscopes, pressure sensors, and magnetic field microsensors.
Another potential application of the magnetic field microsensors is the monitoring of the corrosion and geometrical defects in ferromagnetic pipeline. Fig. 16 depicts an inspection platform for oil pipeline walls reported by Nestleroth & Davis (2007). It is integrated by a rotating permanent magnetic exciter, which may induce uniform eddy currents in the pipe wall. The eddy currents are deflected pipeline defects such as corrosion and axially sligned cracks. The variation of the current densities (that causes a magnetic flux leakage in the pipe wall) could be measured by magnetic field microsensors. Therefore, the defects location could be reached with these microsensors.

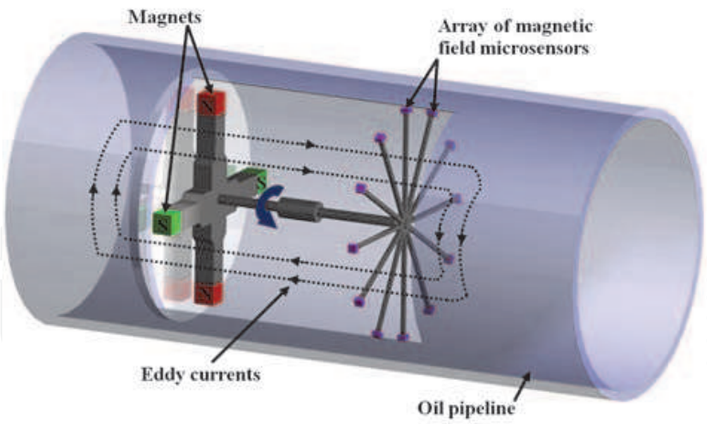

Fig. 16. Schematic view of an inspection platform of oil pipeline walls that consists of a rotating permanent magnetic exciter and an array of magnetic field microsensors.

Magnetic field microsensors could detect cracks, geometrical defects or stress concentration zones in ferromagnetic structures using passive magnetic techniques such as Metal Magnetic Memory (MMM). This technique relies on the self magnetization of ferromagnetic structures by ambient magnetic fields such as the Earth's field (Wilson et al., 2007). It measures changes in the self magnetic leakage field of the ferromagnetic structures due to geometrical discontinuities and high density dislocations.
New cell phones could use resonant magnetic field microsensors, accelerometers, and gyroscopes integrated on a single chip for their global positioning system (GPS). This could reduce the size, cost, and power consumption of the cell phones.
The important advantages of resonant magnetic field microsensors will allow their incorporation in future commercial markets, principally into the automotive sector, telecommunications, and consumer electronics products.

4. Conclusion

The development of resonant magnetic field microsensors based on MEMS has been presented. These microsensors exploit the Lorentz force for measuring magnetic fields and can use different sensing types such as: capacitive, optical, or piezoresistive. Their main advantages are small size, compact structure, light weight, low power consumption, high sensitivity, and high resolution. Most microsensors with piezoresistive detection have had an easy signal processing and a straightforward fabrication process. However, temperature fluctuations have affected their performance. Optical readout systems have allowed microsensors with a reduction in the electronic circuitry and immunity to electromagnetic interference. Microsensors with capacitive sensing have presented little dependence on the temperature, but have needed vacuum packaging and complex electronic circuitry. Future commercial markets will need multifunctional sensors on a single chip for measuring several parameters such as magnetic field, pressure, acceleration, and temperature. several

5. Acknowledgment

This work was supported by CONACYT through grant 84605. The authors would like to thank B. S. Fernando Bravo-Barrera of LAPEM for his assistance with the SEM images.

6. References

Bahreyni, B. (2006). Design, Modeling, Simulating, and Testing of Resonant Micromachined Magnetic Field Sensors. Ph. D. Thesis, University of Manitoba, Winnipeg, Canada.

Bahreyni, B. & Shafai, C. (2007). A Resonant Micromachined Magnetic Field Sensor. IEEE Sensors Journal, Vol. 7, No. 9, (September 2007), pp. 1326-1334, ISSN 1530-437X.

Baschirotto, A.; Borghetti, F.; Dallago, E.; Malcovati, P.; Marchesi, M.; Melissano, E.; Siciliano, P. & Venchi, G. (2006). Fluxgate Magnetic Sensor and Front-End Circuitry in a Integrated Microsystem. Sensors and Actuators A, Vol. 132, No. 1, (November 2006), pp. 90-97, ISSN 0924-4247.

Beeby, S.; Ensell, G.; Kraft, M. & White, N. (2004). MEMS Mechanical Sensors, Artech House, ISBN 978-1-58053-536-6, Norwood, USA.

Beroulle, V.; Bertrand, Y.; Latorre, L. & Nouet, P. Monolithic Piezoresistive CMOS Magnetic Field Sensors. Sensors and Actuators A, Vol. 103, No. 1-2, (January 2003), pp. 23-32, ISSN 0924-4247.

Brugger, S. & Paul, O. (2009). Field-Concentrator-Based Resonant Magnetic Sensor With Integrated Planar Coils. Journal of Microelectromechanical Systems, Vol. 18, No. 6, (December 2009), pp. 1432-1443, ISSN 1057-7157.

Che, L.; Xiong, B.; Li, Y. & Wang, Y. (2010). A Novel Electrostatic-Driven Tuning Fork Micromachined Gyroscope With a Bar Structure Operating at Atmospheric Pressure. Journal of Micromechanics and Microengineering, Vol. 20, No. 1, (January 2010), pp. 015025, ISSN 0960-1317.

Clark, S. K. & Wise, K. D. (1979). Pressure Sensitivity in Anisotropically Etched Thin-Diaphragm Pressure Sensors. IEEE Transactions Electron Devices, Vol. 26, No. 12, (December 1979), pp. 1887-1896, ISSN 0018-9383.

Darrin, M. A. G. (2006). Impact of Space Environment Factors on Microtechnologies, In: MEMS and Microstructures in Aerospace Applications, R. Osiander, M. A. G. Darrin & J. L. Champion, (Eds.), pp. 67-82, Taylor & Francis Group, ISBN 978-0-8247-2637-9, Boca Raton, USA.

Diaz-Michelena, M. (2009). Small Magnetic Sensors for Space Applications. Sensors, Vol. 9, No. 4, pp. 2271-2288, ISSN 1424-8220.

Emmerich, H. & Schöfthaler, M. (2000). Magnetic Field Measurement With a Novel Surface Micromachined Magnetic-Field Sensor. IEEE Transactions on Electron Devices, Vol. 47, No. 5, (May 2000), pp. 972-977, ISSN 0018-9383.

Gad-el-Hak, M. (2001). Introduction, In : The MEMS Handbook, M. Gad-el-Hak, (Ed.), ch. 1, CRC Press, ISBN 9780849321061, Florida, USA.

Hao, Z.; Erbil, A. & Ayazi, F. (2003). An Analytical Model For Support Loss in Micromachined Beam Resonators With In-Plane Flexural Vibrations. Sensors and Actuators A, Vol. 109, No. 1-2, (December 2003), pp. 156-164, ISSN 0924-4247.

Herrera-May, A. L.; Aguilera-Cortés, L. A. ; García-Ramírez, P. J. & Manjarrez, E. (2009a). Resonant Magnetic Field Sensors Based on MEMS Technology. Sensors, Vol. 9, No. 10, (September 2009), pp. 7785-7813. ISSN 1424-8220.

Herrera-May, A. L.; García-Ramírez, P. J. ; Aguilera-Cortés, L. A.; Martínez-Castillo, J. Sauceda-Carvajal, A.; García-González, L. & Figueras-Costa, E. (2009b). A Resonant Magnetic Field Microsensor With High Quality Factor at Atmospheric Pressure. Journal of Micromechanics and Microengineering, Vol. 19, No. 1, (January 2009), pp. 015016, ISSN 1057-7157.

Herrera-May, A. L.; García-Ramírez, P. J.; Aguilera-Cortés, L. A.; Figueras, E.; Martínez-Castillo, J.; Manjarrez, E.; Sauceda, A.; García-González, L. & Juárez-Aguirre, R.

(2011). Mechanical Design and Characterization of a Resonant Magnetic Field Microsensor With Linear Response and High Resolution. Sensors and Actuators A, Vol. 165, No. 2, (February 2011), pp. 399-409, ISSN 0924-4247.

Hull, R. (1999). Properties of Crystalline Silicon, INSPEC, ISBN 0-85296-933-3, London, UK.

Josephs-Franks, P.; Hao, L.; Tzalenchuck, A.; Davies, J.; Kasokova, O.; Gallop, J. C.; Brown, L. & Macfarlane, J. C. (2003). Measurement of the Spatial Sensitivity of Miniature SQUIDs Using Magnetic-Tipped STM. Superconducting Science Technology, Vol. 16, No. 12, (December 2012), pp. 1570-1574, ISSN 0953-2048.

Kádár, Z.; Bossche, A.; Sarro, P. M. & Mollinger, J. R. (1998). Magnetic-Field Measurements Using an Integrated Resonant Magnetic-Field Sensor. Sensors and Actuators A, Vol. 70, No. 3, (October 1998), pp. 225-232, ISSN 0924-4247.

Keplinger, F.; Kvasnica, S.; Hauser, H. & Grössinger, R. (2003). Optical Readouts of Cantilever Bending Designed For High Magnetic Field Application. IEEE Transactions on Magnetics, Vol. 39, No. 5, (September 2003), pp. 3304-3306, ISSN 0018-9464.

Keplinger, F.; Kvasnica, S.; Jachimowicz, A.; Kohl, F.; Steurer, J. & Hauser, H. (2004). Lorentz Force Based Magnetic Field Sensor With Optical Readout. Sensors and Actuators A, Vol. 110, No. 1-3, (February 2004), pp. 112-118, ISSN 0924-4247.

Lenz, J. & Edelstein, A. S. (2006). Magnetic Sensors and Their Applications. IEEE Sensors Journal, Vol. 6, No. 3, (June 2006), pp. 631-649, ISSN 631-649.

Li, P. & Fang, Y. (2009). A New Free Molecular Model for Squeeze-Film Damping of Flexible Microbeam in Low Vacuum. Micro and Nanosystems, Vol. 1, No. 1, (March 2009), pp., ISSN 1876-4029.

Li, L.; Stankovic, V.; Stankovic, L.; Li, L.; Cheng, S. & Uttamchandani, D. (2011). Single Pixel Optical Imaging Using a Scanning MEMS Mirror. Journal of Micromechanics and Microengineering, Vol. 21, No. 2, (February 2011), pp. 025022, ISSN 1057-7157.

Li, Y.; Zheng, Q.; Hu, Y. & Xu, Y. (2011). Micromachined Piezoresistive Accelerometer Based on a Asymmetrically Gapped Cantilever. Journal of Microelectromechanical Systems, Vol. 20, No. 1, (February 2011), pp. 83-94, ISSN 1057-7157.

Mian, A. & Law, J. (2010). Geometric Optimization of a Van Der Pauw Structure Based MEMS Pressure Sensor. Microsystem Technologies, Vol. 16, No. 11, (November 2010), pp. 1921-1929, ISSN 0946-7076.

Mohammadi, A. R.; Graham, T. C. M.; Bennington, C. P. J. & Chiao M. (2010). Development of a Composated Capacitive Pressure and Temperature Sensor Using Adhesive Bonding and Chemical-Resistant Coating for Multiphase Chemical Reactors. Sensors and Actuators A, Vol. 163, No. 2, (October 2010), pp. 471-480, ISNN 0924-4247.

Mohammadi, A. R.; Bennington C. P. J. & Chiao M. (2011a). Development of a Combined Piezoresistive Pressure and Temperature Sensor Using a Chemical Protective Coating for Kraft Pulp Digester Process Monitoring. Journal of Micromechanics and Microengineering, Vol. 21, No. 1, (January 2011), pp. 015009, ISSN 1057-7157.

Mohammadi, A. R.; Bennington C. P. J. & Chiao M. (2011b). A Hybrid Capacitive Pressure and Temperature Sensor Fabricated by Adhesive Bonding Technique for Harsh Enviroment of Kraft Pulp Digesters. Microsystem Technologies, Vol. 17, No. 1, (January 2011), pp. 149-160, ISSN 0946-7076.

Nestleroth, J. B. & Davis, R. J. (2007). Application of Eddy Currents Induced by Permanent Magnets For Pipeline Inspection. NDT & International, Vol. 40, No. 1, (January 2007), pp. 77-84, ISSN 0963-8695.

Perez, L.; Aroca, C.; Sánchez, P.; López, E. & Sánchez, M. C. (2004). Planar Fluxgate Sensor With an Electrodeposited amorphous core. Sensors and Actuators A, Vol. 109, No. 3, (January 2004), pp. 208-211, ISSN 0924-4247.

Popovic, R. S. (2004). Hall Effect Devices, (2nd ed.), Institute of Physics Publishing, ISBN 0-7503-0855-9, Bristol, USA.

Ren, D.; Wu, L.; Yan, M.; Cui, M.; You, Z. & Hu, M. (2009). Design and Analysis of a MEMS Based Resonant Magnetometer. Sensors, Vol. 9, No. 9, (September 2009), pp. 6951-6966, ISSN 1424-8220.

Ripka, P. (2000). New Directions in Fluxgate Sensors. Journal of Magnetism and Magnetic Materials, Vol. 215-216, No. 2, (June 2000), pp. 735-739, ISSN 0304-8853.

Ripka, P. & Tipek, A. (2007). Modern Sensors Handbook, ISTE Ltd, ISBN 9781905209668, Wiltshire, UK.

Ripka, P. (2008). Improvening the accuracy of magnetic sensors, In: Sensors: Advancements in Modeling, Design Issues, Fabrication and Practical Applications, S. C. Mukhopadhyay & R. Y. M. Huang, (Eds.), 45-60, Springer-Verlag, ISBN 978-3-540-69030-6, Berlin, Germany.

Sunier, R.; Vancura, T.; Li, Y.; Kay-Uwe, K.; Baltes, H. & Brand, O. (2006). Resonant Magnetic Field Sensor With Frequency Output. Journal of Microelectromechanical Systems, Vol. 15, No. 5, (Octuber 2006), pp. 1098-1107, ISSN 1057-7157.

Tapia, J. A.; Herrera-May, A. L.; García-Ramírez, P. J.; Martínez-Castillo, J.; Figueras, E.; Flores, A. & Manjarrez, E. (2011). Sensing Magnetic Flux Density of Artifical Neurons With a MEMS Device. Biomedical Microdevices, Vol. 13, No. 2, (April 2011), pp. 303-313, ISSN 1387-2176

Tucker, J.; Wesoleck, D. & Wickenden, D. (2002). An Integrated CMOS MEMS Xylophone Magnetometer With Capacitive Sense Electronics, NanoTech 2002, pp. 5723, Houston, Texas, USA, September 9-12, 2002.

Tunvir, K.; Ru, C. Q. & Mioduchowski, A. (2010). Thermoelastic Dissipation of Hollow Micromechanical Resonators. Physica E: Low-dimensional Systems and Nanostructures, Vol. 42, No. 9, (July 2010), pp. 2341-2352, ISSN 1386-9477.

Vengallatore, S. (2005). Analysis of Thermoelastic Damping in Laminated Composite Micromechancial Beam Resonators. Journal of Micromechanics and Microengineering, Vol. 15, No. 12, (December 2005), pp. 2398-2404, ISSN 1057-7157.

Wang, Q.; Li, X.; Li, T.; Bao, M. & Zhou, W. (2011). On-Chip Integration of Acceleration, Pressure, and Temperature Composite Sensor With a Single-Sided Micromachining Technique. Journal of Microelectromechanical Systems, Vol. 20, No. 1, (February 2011), pp. 42-52, ISSN 1057-7157.

Watanabe, H.; Yamada, N. & Okaji, M. (2004). Linear Thermal Expansion Coefficient of Silicon From 293 to 1000 K. International Journal of Thermophysics, Vol. 25, No. 1, (January 2004), pp. 221-236, ISSN 0195-928X.

Wickenden, D. K.; Chamption, J. L.; Osiander, R.; Givens, R. B.; Lamb, J. L.; Miragliotta, J. A.; Oursler, D. A. & Kistenmacher, T. J. (2003). Micromachined Polysilicon Resonating Xylophone Bar Magnetometer. Acta Astronautica, Vol. 52, No. 2-6, (January-March 2003), pp. 421-425, ISSN 0094-5765.

Wilson, J. W., Tian, G. Y. & Barrans, S. (2007). Residual Magnetic Field Sensing For Stress Measurement. Sensors and Actuators A, Vol. 135, No. 2, (April 2007), pp. 381-387, ISSN 0924-4247.

Zanetti, L. J.; Potemra, T. A.; Oursler, Lohr, D. A.; Anderson, B. J.; Givens, R. B.; Wickenden, D. K.; Osiander, R.; Kistenmacher, T. J. & Jenkins, R. E. (1998). Miniature Magnetic Field Sensors Based on Xylophone Resonators, In: Science Closure and Enabling Technologies for Constellation Class Missions, V. Angelopoulos & P. V. Panetta, (Eds.), 149-151, University of California Press, ISBN 0-9670138-0-1, CA, USA.

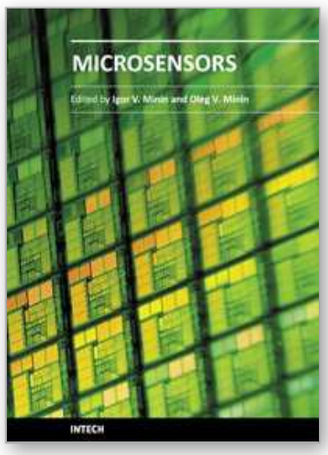

Microsensors

Edited by Prof. Igor Minin

ISBN 978-953-307-170-1
Hard cover, 294 pages
Publisher InTech
Published online 09, June, 2011
Published in print edition June, 2011

This book is planned to publish with an objective to provide a state-of-art reference book in the area of microsensors for engineers, scientists, applied physicists and post-graduate students. Also the aim of the book is the continuous and timely dissemination of new and innovative research and developments in microsensors. This reference book is a collection of 13 chapters characterized in 4 parts: magnetic sensors, chemical, optical microsensors and applications. This book provides an overview of resonant magnetic field microsensors based on MEMS, optical microsensors, the main design and fabrication problems of miniature sensors of physical, chemical and biochemical microsensors, chemical microsensors with ordered nanostructures, surface-enhanced Raman scattering microsensors based on hybrid nanoparticles, etc. Several interesting applications area are also discusses in the book like MEMS gyroscopes for consumer and industrial applications, microsensors for non invasive imaging in experimental biology, a heat flux microsensor for direct measurements in plasma surface interactions and so on.

How to reference

In order to correctly reference this scholarly work, feel free to copy and paste the following:

Agustín L. Herrera-May, Luz A. Aguilera-Cortés, Pedro J. García-Ramírez, Nelly B. Mota-Carrillo, Wendy Y. Padrón-Hernández and Eduard Figueras (2011). Development of Resonant Magnetic Field Microsensors: Challenges and Future Applications, Microsensors, Prof. Igor Minin (Ed.), ISBN: 978-953-307-170-1, InTech, Available from: http://www.intechopen.com/books/microsensors/development-of-resonant-magnetic-field-microsensors-challenges-and-future-applications

INTECH
open science | open minds

InTech Europe
University Campus STeP Ri
Slavka Krautzeka 83/A
51000 Rijeka, Croatia
Phone: +385 (51) 770 447
Fax: +385 (51) 686 166
www.intechopen.com

InTech China
Unit 405, Office Block, Hotel Equatorial Shanghai
No.65, Yan An Road (West), Shanghai, 200040, China
中国上海市延安西路65号上海国际贵都大饭店办公楼405单元
Phone: +86-21-62489820
Fax: +86-21-62489821

IntechOpen